Structure, Vol. 9, 897–904, October, 2001, ©2001 Elsevier Science Ltd. All rights reserved. PII S0969-2126(01)00657-8

Structure of a Conjugating Enzyme-Ubiquitin Thiolester Intermediate Reveals a Novel Role for the Ubiquitin Tail

Katherine S. Hamilton,[1,5] Michael J. Ellison,[1,2,4] Kathryn R. Barber,[3] R. Scott Williams,[1] John T. Huzil,[1] Sean McKenna,[1] Christopher Ptak,[1] Mark Glover,[1,2] and Gary S. Shaw[3,4]

[1]Department of Biochemistry
[2]Institute for Biomolecular Design
The University of Alberta
Edmonton, Alberta T6G 2H7
Canada

[3]Department of Biochemistry and R.S. McLaughlin Macromolecular Structure Facility
The University of Western Ontario
London, Ontario N6A 5C1
Canada

Summary

Background: Ubiquitin-conjugating enzymes (E2s) are central enzymes involved in ubiquitin-mediated protein degradation. During this process, ubiquitin (Ub) and the E2 protein form an unstable E2-Ub thiolester intermediate prior to the transfer of ubiquitin to an E3-ligase protein and the labeling of a substrate for degradation. A series of complex interactions occur among the target substrate, ubiquitin, E2, and E3 in order to efficiently facilitate the transfer of the ubiquitin molecule. However, due to the inherent instability of the E2-Ub thiolester, the structural details of this complex intermediate are not known.

Results: A three-dimensional model of the E2-Ub thiolester intermediate has been determined for the catalytic domain of the E2 protein Ubc1 ($Ubc1_{\Delta 450}$) and ubiquitin from *S. cerevisiae*. The interface of the E2-Ub intermediate was determined by kinetically monitoring thiolester formation by ^{1}H-^{15}N HSQC spectra by using combinations of ^{15}N-labeled and unlabeled $Ubc1_{\Delta 450}$ and Ub proteins. By using the surface interface as a guide and the X-ray structures of Ub and the 1.9 Å structure of $Ubc1_{\Delta 450}$ determined here, docking simulations followed by energy minimization were used to produce the first model of a E2-Ub thiolester intermediate.

Conclusions: Complementary surfaces were found on the E2 and Ub proteins whereby the C terminus of Ub wraps around the E2 protein terminating in the thiolester between C88 ($Ubc1_{\Delta 450}$) and G76 (Ub). The model supports in vivo and in vitro experiments of E2 derivatives carrying surface residue substitutions. Furthermore, the model provides insights into the arrangement of Ub, E2, and E3 within a ternary targeting complex.

[4]Correspondence: shaw@serena.biochem.uwo.ca (G.S.S.), mike.ellison@ualberta.ca (M.J.E.)
[5]Present address: Department of Chemistry, Acadia University, Wolfville, Nova Scotia B0P 1X0, Canada.

Introduction

The selective targeting of proteins for degradation by ubiquitination regulates an impressive array of processes that include cell cycle regulation, transcription, and oncogenesis [1]. The common denominator of these processes is the initial C-terminal activation of ubiquitin (Ub) by the activating enzyme (E1) followed by its subsequent transfer to a Ub-conjugating enzyme (E2) as a covalent E2-Ub thiolester intermediate. At this point, the mechanism of ubiquitination appears to diverge along either of two lines. In one case, Ub is transferred directly from the E2 to the lysine of a target protein in a reaction that is facilitated by a Ub protein ligase (E3). In the other case, Ub is first transferred from the E2 to the active site cysteine of an E3 as an E3-Ub thiolester intermediate, whereupon it is then transferred to the target protein. In either event, degradation of the target by the 26S proteasome is facilitated by the assembly of a multi-Ub chain on the target in which the C terminus of each Ub is linked to Lys48 (K48) of its neighbor.

The ability of E2 proteins to orchestrate ubiquitination through their interactions with Ub, E1, E3, and target proteins makes them central players of the ubiquitin cascade. All E2 proteins consist of a catalytic domain (150 residues) that includes the active site cysteine used to form the E2-Ub thiolester complex. Furthermore, X-ray crystallographic structures of the catalytic domains from the E2 proteins Ubc1 (vide infra), Ubc2 [2], Ubc7 [3], and Ubc9 [4] from *Saccharomyces cerevisiae* have shown that this region is structurally conserved. Four α helices (α1–α4) essentially form one face of the protein, while a 4 strand antiparallel β sheet (β1–β4) is found on the backside of the enzyme between helices α1 and α2 in the sequence. The thiolester-forming cysteine is located on a relatively unstructured region (L2) ranging from 20 to 30 residues in length and linking β4 and α2. Recent X-ray crystallographic studies have shown that two structurally unrelated E3 proteins, E6AP and cCbl, interact with the E2 protein UbcH7 at similar positions [5, 6]. Specifically, the E3 proteins interact with mainly hydrophobic residues just prior to the α2 helix in the L2 region and between β strands β3 and β4 in the L1 region. Furthermore, electrostatic interactions occur with residues along the face of the N-terminal α1 helix in UbcH7. Based on this positioning of the two proteins, it has been suggested that E3 proteins function as scaffolds, allowing optimal transfer of the ubiquitin from the E2 protein to the targeted substrate. However, the mechanism for this transfer remains unclear largely because the structural characterization of the predecessor to this complex, the E2-Ub thiolester, has proven to be more elusive. In vitro the E2-Ub thiolester can be formed with a high conversion [7]. However, the complex undergoes facile hydrolysis, yielding the original precursor proteins.

Key words: ubiquitination; protein-protein interactions; protein degradation; covalent complex; NMR spectroscopy; X-ray crystallography

Therefore, the transient nature of the E2-Ub thiolester intermediate precludes its three-dimensional determination by either NMR spectroscopy or X-ray crystallography. In the present work we have used NMR spectroscopy to identify the interfacial residues of the E2-Ub thiolester intermediate derived from *S. cerevisiae*. These results were combined with computer-aided molecular modeling to determine the first three-dimensional model of an E2-Ub thiolester complex. The validity of the model was reinforced by biological experiments aimed at uncovering the importance of particular residues in the ubiquitination pathway. The structure reveals a first glimpse of the surface recognition site between the Ub and E2 proteins and provides insight into the three-dimensional arrangement of Ub, E2, and E3 in the ternary complex.

Results and Discussion

Several attempts have been made to determine the three-dimensional structures of E2-Ub and related complexes by using NMR spectroscopy. Noncovalent complexes of ubiquitin, with the C-terminal hydrolase proteins UCH-L3 [8] and YUH-1 [9], have allowed a partial map of the surfaces on the hydrolase enzyme to be probed. The nature of the E2-Ub complex has also been studied for the noncovalent complex between the E2 protein Ubc9 and a ubiquitin homolog (UBL1) [10]. These two studies indicated that a broad surface on the E2 protein could be mapped by using NMR chemical-shift perturbation methods and, in the case of UCH-L3, a model was suggested for its interactions with ubiquitin. Chemical-shift perturbation methods have been used to identify the interacting surfaces in a covalent complex between the human E2 protein Ubc2b and ubiquitin [11]. However, the instability of the complex and its tendency to associate in the absence of thiolester bond formation hindered attempts to dock the two proteins and to produce a model of the E2-Ub complex.

Our previous studies have shown that the E2-Ub thiolester intermediate can be created from Ub and the E2 catalytic domain from Ubc1 ($Ubc1_{\Delta 450}$ residues 1–150; residues 151–215 are deleted) from *S. cerevisiae* [7, 12]. The reaction utilizes a catalytic cocktail comprising E1 (*S. cerevisiae*), Mg^{2+}, and ATP and can be scaled up to millimolar concentrations that are required for NMR experiments where the E2-Ub complex can be assembled in situ, in the NMR tube. Appropriate amino acid substitutions have been introduced into Ub (K48R) and $Ubc1_{\Delta 450}$ (K93R) to eliminate autoubiquitination of $Ubc1_{\Delta 450}$ and the formation of multiubiquitin chains, which are two complicating side products of the reaction. The E2-Ub intermediate is sufficiently labile to preclude its three-dimensional structure by either NMR or X-ray crystallographic techniques. Unlike the noncovalent complexes of Ubc9 with UBL1 protein [10], UCH-L3 with Ub protein [8], and Ubc2b with Ub [11] protein, there is no observable association of $Ubc1_{\Delta 450}$ and Ub in solution at the NMR concentrations studied and in the absence of the activating enzyme E1, ATP, and Mg^{2+}. ^{1}H-^{15}N HSQC spectra of solutions of the individual proteins were virtually indistinguishable from spectra containing both proteins but in the absence of the catalytic cocktail.

Footprint of the E2-Ub Interaction

A series of ^{1}H-^{15}N HSQC spectra were used to monitor the formation of the E2-Ub thiolester intermediate. Spectra were acquired as a function of time from two reactions that contained catalytic amounts of E1 with either (1) ^{15}N-Ub and unlabeled E2 or (2) ^{15}N-E2 and unlabeled Ub. In the NMR tube, the reaction could be conveniently monitored by ^{1}H-^{15}N HSQC spectra taken at 1 min intervals and reached approximately 90% completion as determined by gel fitration chromotography. Building upon the NMR assignments of the uncomplexed forms of the proteins [12, 13], we used the changes in crosspeak intensity as a measure of thiolester formation. We used this method rather than the usual change in chemical shift method because small environmental changes were inevitable during the in situ NMR reactions, and Ub has been shown to be very pH sensitive [12]. Figure 1 shows a comparison for regions of ^{1}H-^{15}N HSQC spectra for the ^{15}N-Ub and ^{15}N-E2 proteins in the free (Figures 1a and 1c) and thiolester (Figures 1b and 1d) forms. Upon E2-Ub thiolester formation (Figures 1b and 1d), there is a general decrease in peak intensities resulting from the increased molecular weight of the covalent intermediate (24 kDa) compared to that of the E2 (16 kDa) or Ub (8 kDa) proteins by themselves. Furthermore, it is obvious that several resonances have a significantly greater decrease in intensity than others do. As shown in Figures 1a and 1b, these resonances correspond to residues near the C terminus of Ub (V70, L71, R72, and L73) and to those near β strand β3 of the protein (R42, L43, and R48). In addition, the ^{1}H-^{15}N resonance for the thiolester-forming residue G76 was visibly absent from the spectrum of the E2-Ub complex (data not shown). These observations correlate well with those of the noncovalent UCH-L3-Ub [8] and thiolester Ubc2b-Ub [11] complexes where regions 4–14, 39–50, and 67–76 (in UCH-L3-Ub) and regions 7–9, 40–49, and 70–76 (in Ubc2b-Ub) of Ub were noted to have the most significant chemical shift changes upon complex formation. These results suggest that some common residues in Ub may be important for protein interactions with E2 proteins and with ubiquitin hydrolase proteins.

Figures 1c and 1d show a representative sampling of residues that decreased in peak intensity by >90% for the E2 protein. Amongst these were residues in the linker region between β strand β4 and helix α2, including the active site residue C88 and residues K74, V75, S82, L89, and I100. Other residues in this region that underwent similar intensity decreases (data not shown) included N79, I80, S81, Y83, I87, L91, L92, W96, and S97. Several residues in helix α2 (A105, S108, and Q114), in the following linker (S115 and N119), and in the N terminus of α1 (R3) were affected significantly by E2-Ub thiolester formation. Residues such as I87–I91 are similar to those observed in the formation of a thiolester complex between human E2b and ubiquitin [11]. However, we noted that $Ubc1_{\Delta 450}$ had many affected residues including A105, S108, and Q114 in helix α2 and S115 or N119 in the following linker that were not observed to change significantly in the E2b protein upon complex formation. Similarly, the residues identified in the present work with $Ubc1_{\Delta 450}$ do not correlate well with those identified in the noncovalent interaction of the E2 protein Ubc9

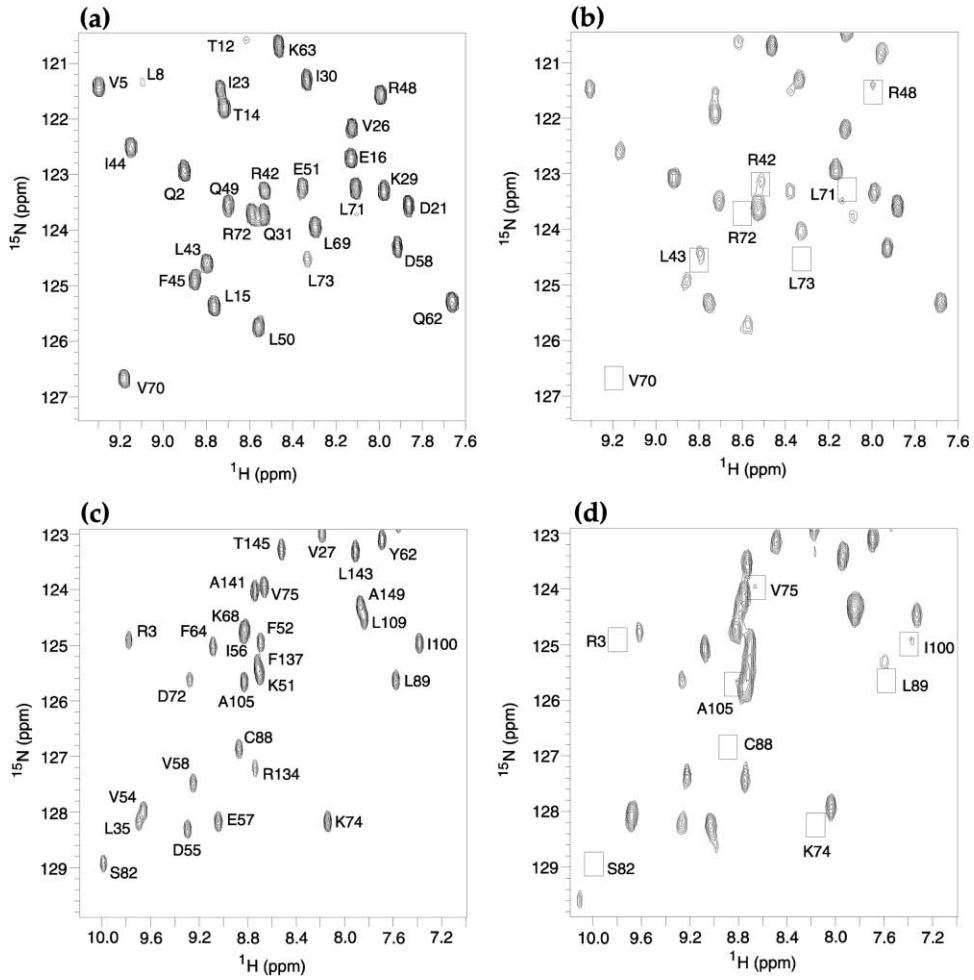

Figure 1. E2-Ub Thiolester Formation Probed by NMR Spectroscopy

Selected regions of 500 MHz ^{1}H-^{15}N HSQC spectra of ^{15}N-Ub (a and b) and ^{15}N-E2 (c and d) showing the effect of thiolester formation on peak intensity. Spectrum (a) shows 0.8 mM ^{15}N-Ub and 0.8 mM unlabeled E2 collected prior to thiolester formation in 40 mM HEPES, 450 mM NaCl, and 1 mM EDTA (pH 7.5). The sample volume was reduced and 10 μM E1, 10 mM ATP, and 5 mM MgCl added to initiate thiolester formation. The resulting ^{1}H-^{15}N HSQC spectrum of the thiolester is shown in (b) after approximately 1 hr of reaction. An identical experiment is shown for 0.8 mM ^{15}N-labeled E2 prior to thiolester formation (c) and 1 hr after thiolester formation with unlabeled Ub (d). In both cases resonances are indicated with boxes (b and d) to indicate those that decreased in intensity >90% when compared to those prior to thiolester formation (a and c).

with the ubiquitin-like protein UBL1 [10]. In that study, several residues on the N-terminal helix of Ubc9, opposite the active site, were identified. Together these results indicate that residues in helix α2 of Ubc1$_{\Delta 450}$ may have unique roles in thiolester formation.

In general, the larger decreases in intensity in E2 and Ub that occurred upon thiolester formation were attributed to a decreased mobility of these residues or to a significant change in environment relative to the remaining portions of the molecules. These observations could be consistent with the placement of these residues at the protein-protein interface of the E2-Ub intermediate. In order to test this hypothesis, the residues in E2 and Ub that exhibited the greatest peak intensity decrease upon thiolester formation were mapped to the X-ray crystallographic surfaces of Ub [14] and the catalytic domain of the E2 from *S. cerevisiae*, Ubc1$_{\Delta 450}$, reported here to 1.9 Å resolution (Figure 2; Table 1). For clarity, two cutoff points were selected: a >90% decrease in peak intensity, and a peak-intensity decrease between 79% and 90%. This latter group was chosen because it represented residues that still decreased by 5 times their original amplitude and more than double that expected from a simple molecular-weight size increase in the E2-Ub covalent complex. Figure 2 shows the majority of affected residues are clustered together with their side chains exposed to the exterior of each protein. In the case of E2 (Figure 2a), several residues face toward a cleft in the protein formed between two 3 residue β sheets and a 3 residue helix in the linker on one side and helix α2 on the other side. These include residues N79, I80, and S81 in α5 and residues I87 and the thiolester-forming C88 in β6. The residues in helix α2 include A105 and S108 that point down toward the

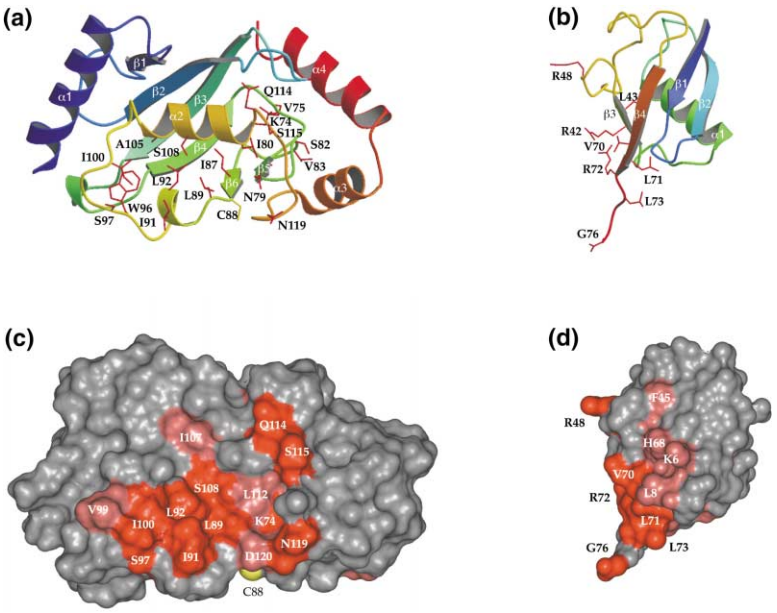

Figure 2. Surfaces of Interaction in the E2-Ub Thiolester Intermediate

Ribbon presentation of (a) the 1.9 Å structure of the Ubc1 catalytic domain (E2) and (b) Ub-depicting side chains for residues that were most affected by thiolester formation. Side chains are shown in red for residues that had a peak intensity decrease of >90% in ^{1}H-^{15}N HSQC spectra as compared to spectra of the uncomplexed proteins. Connolly surface presentation of (c) E2 and (d) Ub corresponding to (a) and (b) above and depicting surfaces comprising residues affected most by thiolester formation. Surfaces colored red indicate residues in E2 and Ub as in (a) and (b) above. Surfaces are also colored (magenta) to indicate those residues whose peak intensities decreased between 10% and 16% (Ub) and between 10% and 21% (E2) as compared to the uncomplexed forms of these proteins.

cavity and Q114 and S115 that point out toward the solvent. It is interesting that two residues, N79 and W96, are also perturbed. These residues are completely conserved in the *S. cerevisiae* family of E2 proteins [3]. Structurally, the side chain amide of N79 forms a hydrogen bond to the backbone NH of the catalytic C88. Likewise, W96 makes important hydrophobic contacts with Y62, P67, I100, and L92. Thus, the changes in intensities of these two residues appear to be transmitted by thiol formation with C88 (N79) and by a possible reorientation of the linker (W96) rather than by direct interaction with the ubiquitin molecule. In the case of Ub (Figure 2b), residues nearby in β sheet β3 (R42, L43, and R48) and in the tail region of the protein (L71, R72, and L73), including the thiolester-forming G76, point out toward the solvent. It is likely that residues R74 and G75 are part of this group. However, neither could be observed in Ub due to rapid amide exchange with solvent. Only one residue, L43, is oriented in the opposite direction.

The residues identified in Figures 2a and 2b and those displaying the next cutoff point (79%–90%) were mapped as accessible surfaces in the E2 and Ub proteins (Figures 2c and 2d). For the E2 protein, this approach showed that the surface formed radiates to one side of the molecule leading away from the active site, including C88 (Figure 2c). The side chains from this region cover an accessible surface area of 1369 Å^2, approximately 42% of which is comprised from the side chains of hydrophobic residues. Of these, residues I91 and V99 are prominently displayed on the surface of the protein in this region. For the Ub protein, hydrophobic residues comprise about 32% of the side chain-accessible surface area (1218 Å^2), based on the NMR data. The similarity in side chain-accessible surface areas for E2 and Ub is consistent with these residues forming a common interface between the two proteins.

Table 1. Crystallographic Data and Refinement Statistics

Resolution range (Å)	20–1.9
Number of observed reflections	85,242
Number of unique reflections	23,300
Completeness (%)	97.8 (81.1)[a]
R_{sym} (%)[b]	10.1 (34.5)
$<I/\sigma I>$	15.5 (3.5)
R factor/R_{free} (%)[c]	20.9/24.1
Number of residues/number of H_2O	298/300
Root mean square deviation, bond lengths (Å)	0.009
Root mean square deviation, bond angles (°)	1.27
Ramachandran plot (%):	
Most favored	92.2
Allowed	7.8

[a] Values in parentheses are statistics for the highest resolution shell (1.93–1.90 Å).

[b] $R_{sym} = 100\Sigma_h\Sigma_i| I_i(h) - <I(h)>| / \Sigma_h\Sigma_i I(h)$, for the intensity of i observations of reflection h.

[c] $R_{cryst} = \Sigma_h \mid F_o(h) - F_c(h) \mid / \Sigma_h \mid F_o(h) \mid$, where $F_o(h)$ and $F_c(h)$ are observed and calculated structure factors. R_{free} was calculated with 10% of all reflections excluded from refinement stages by using high-resolution data.

Structure of the E2-Ub Intermediate

The E2-Ub footprint obtained from ^{1}H-^{15}N HSQC experiments and shown in Figures 2c and 2d was used in combination with multiple separate Monte Carlo calculations to dock the two proteins. Initial docking experiments were done without the thiolester linkage present. However, since the final E2-Ub complex possesses this covalent bond between C88 (E2) and G76 (Ub), this greatly aided the docking procedure and limited the number of E2-Ub complex possibilities. The lowest-energy combinations of these structures had the C-terminal tail from Ub wrapped around the E2 protein with G76 pointed toward the active site C88 residue of E2. A modest conformational adjustment of the crystallographic form of Ub was required to produce the covalent bond that links the E2 C88 thiol to the Ub C-terminal carboxylate to form the thiolester. This modification was not surprising, given the significant observed flexibility

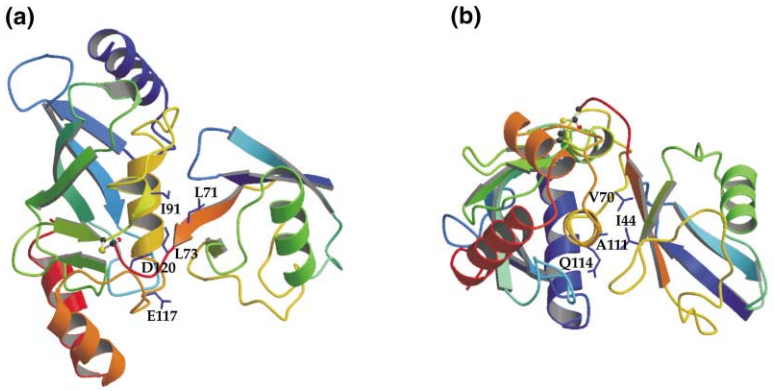

Figure 3. Model of the E2-Ub Thiolester Intermediate

The model was determined by Monte Carlo docking as described in Experimental Procedures. The model shows (a) side and (b) end orientation views of helix $\alpha 2$ in the E2 molecule. Residues are indicated on both E2 and Ub to indicate important side chain-side chain interactions that arise at the protein-protein interface, as described in the text. In both figures, the thiol-forming C88 residue in E2 is a shown as a yellow ball-and-stick representation near the (a) center and (b) top of the complex.

of the Ub C terminus in solution as determined from ^{15}N and ^{13}C relaxation experiments [15, 16]. In the E2-Ub thiolester model (Figure 3), residues L71–G76 from Ub position themselves in a shallow cleft from E2-comprising residues L89–I91 on one side and N119–P121 on the other. This results in stacking interactions of the R72 and R74 side chains from Ub with the side chain of N119 from E2, although direct charge interactions are not apparent. Two important sections of hydrophobic interactions exist; L71 and L73 from Ub sandwich I91 just C-terminal of the active site C88 in the E2 protein, and the side chains of I44 and V70 in Ub lie on opposite sides of A111 βCH_3 in E2. This latter interaction is also supported from interactions with the β,γ CH_2 groups from Q114 of E2. The E2-Ub interface is also supported by several obvious hydrogen bonding interactions between the side chains of E117 (E2) and R72 (Ub), between the side chain of D120 (E2) with G75 NH (Ub), and between A111 CO (E2) with the side chain of R42 (Ub). Together, the side chain interface of the E2-Ub thiolester intermediate occupies approximately 1823 $Å^2$ of surface area comprising about 48% nonpolar components and 52% polar or charged side chains. Furthermore, residues at the interface including I44, V70, L71, and L73 in Ub and A111, Q114, N119, and D120 in E2 were amongst those with the largest peak-intensity changes.

The interacting surface between E2 and Ub is consistent with site-directed mutugenesis experiments. In Ub the tail residues comprising R72–G76 are essential for Ub function [17]. Furthermore, this sequence is completely conserved among all ubiquitin sequences. In the E2-Ub thiolester complex, the side chains of these residues account for nearly 300 $Å^2$ of contact surface at the thiolester interface. With the exception of G75, each residue in the RLRGG region of Ub has $>40\%$ of its side chain buried in the E2-Ub thiolester intermediate as compared to the isolated proteins. Amongst these is R72, shown to be a critical residue (along with R54) for initial E1 binding [18] and for the interaction of Ub with the UCH-L3 hydrolase [8]. In the E2-Ub complex, it appears that R42 rather than R54 is more involved at the E2-Ub interface. These results suggest that R42 may be a distinguishing residue for the interaction in the E2-Ub complex as compared to other Ub complexes.

Other similarities exist between the residues involved at the E2-Ub interface and residues important for E1 function. For example, residues L8, I44, and V70 in Ub are all proposed as important for E1 binding [19]. These residues also make intimate contacts in the E2-Ub thiolester complex. Furthermore, these residues also form a repeating surface patch in polyubiquitin chains implicated in binding to the 26S proteosome.

The interacting surface for E2 contains two residues (S97 and A111) that are important to its function. The replacements of S97R and A111R in $Ubc1_{\Delta 450}$ both result in an E2 that retains full capacity for thiolester formation but has lost its stress-related function in vivo. In addition, the A111R replacement strongly attenuates the E2's ability to catalyze multi-Ub chains in vitro (M.J.E., unpublished data). However, these substitutions have no effect on the catalytic transfer of Ub from E1 to E2. Therefore, the position occupied by Ub on the E2 surface is only required for downstream functions such as multi-Ub chain assembly and target recognition. Conversely, the replacements T73R and K74A in $Ubc1_{\Delta 450}$ occur at amino acid positions that are not at the E2-Ub interface in the thiolester. These substitutions have no effect on thiolester formation, chain assembly, or the E2's in vivo properties (data not shown).

A Glimpse at the E3-E2-Ub Ternary Complex

The structural relationship between the E2-Ub thiolester intermediate and the Ub protein ligases (E3 proteins) is an important prerequisite for understanding the mechanistic events leading to target-substrate recognition. There have recently been two structural reports of E2-E3 complexes. One complex is composed of the E2 protein HsUbc7 and the E3 protein E6AP, a member of the HECT class of E3s [5]. The other complex is composed of HsUbc7 and the E3 protein c-Cbl, a member of the RING-finger class of E3s [6]. In both cases, specific and nearly identical noncovalent interactions occur between the E3 protein and the L1 (F57–P65) and L2 (W95–K100) loop regions of the E2 protein. Specifically, residues A59, E60, P62, F63, and K64 (L1) and K96, P97, A98, and K100 (L2) make close contacts with the E3 proteins. Further charge-charge contacts exist between R6 and K9 in helix $\alpha 1$ of the E2 protein and E3.

Based on the E2-E3 X-ray structures, it has been suggested that the sequences of the L1 and L2 loops in the E2 proteins define the specificity for interaction with an E3 protein [5]. Analysis of these regions in Ubc1 indicates a very high conservation between UbcH7 and

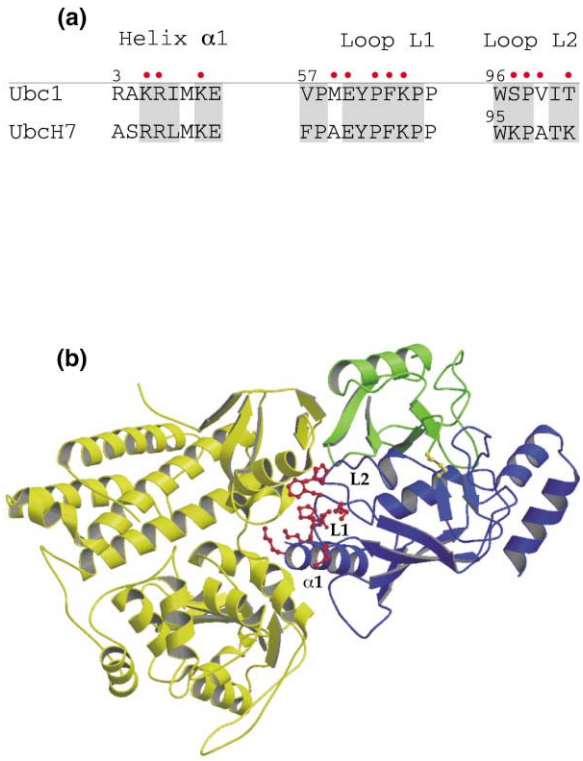

Figure 4. Model and Rationale for an E3-Ubc1$_{\Delta 450}$-Ub Ternary Complex

(a) Sequence comparison of Ubc1$_{\Delta 450}$ and UbcH7 for helix α1 and loops L1 and L2. Key intermolecular contacts between UbcH7 and both c-Cbl and the HECT E3 E6AP, and those proposed to occur for Ubc1 are indicated by dots above the sequence. Residues that are conserved in UbcH7, Ubc1, and other E2 proteins that interact with HECT or c-Cbl E3 proteins are shaded.

(b) Proposed ternary complex of E3-Ubc1$_{\Delta 450}$-Ub. The model was produced by superposition of residues with defined secondary structure in Ubc1$_{\Delta 450}$ (4–17, 22–26, 34–41, 50–58, 67–72, 104–113, 123–132, and 135–147) in the E2-Ub model presented here with the corresponding regions of UbcH7 in the UbcH7-c-Cbl complex derived from X-ray crystallography. The rmsd for this superposition was 3.0 Å. The structure of UbcH7 was subsequently removed. Residues proposed to be located at the E2-E3 interface in Ubc1 are indicated. The molecule colors are blue for Ubc1, green for Ub, and lime for c-Cbl.

Ubc1$_{\Delta 450}$ (Figure 4a). In particular, F63, a residue known to be critical for HECT domain and c-Cbl-mediated ubiquitination, is conserved [20]. This indicates that interaction of Ubc1$_{\Delta 450}$ with an E3 protein should occur via the same intermolecular surface, although the precise E3 that interacts with Ubc1 has yet to be identified. This structural similarity of Ubc1$_{\Delta 450}$ in the E2-Ub thiolester intermediate and HsUbc7 in the E2-E3 complex allows the spatial relationship of the E2, E3, and Ub components of an E3-E2-Ub thiolester complex to be proposed for a first time. In this manner, such a structure may lend clues for the transfer of Ub between E2 and E3 or between E2 and a target substrate.

In Figure 4b, the three-dimensional structure UbcH7 in the HsUbc7-c-Cbl complex was superimposed with Ubc1$_{\Delta 450}$ in the Ubc1$_{\Delta 450}$-Ub thiolester model described in the current work to provide a picture of the E3-Ubc1$_{\Delta 450}$-Ub ternary complex. Similar to the original crystallographic work, the figure shows that a common interaction between the E3 protein and the E2 protein, Ubc1$_{\Delta 450}$, is maintained. In particular, the E2 interface comprises residues R6 and K9 in helix α1, residues M60, E61, P63, F64, and K65 between strands β3 and β4 (LI region), and residues P98 and V99 prior to helix α2 (L2 region). The model of the E2-Ub thiolester intermediate does not include any of the interactions important for E2-E3 recognition, indicating that the E2 proteins have unique interactions with Ub and E3 proteins. Furthermore, the E3-E2-Ub ternary complex indicates that the Ub molecule is held adjacent to the E3 protein through contacts with E2. This tight association of proteins presents an attractive arrangement for Ub transfer to a target protein recruited by the E3 protein, one of the possible mechanisms for ubiquitin targeting.

Biological Implications

Ubc1 is the yeast E2 protein that plays a key role in the ubiquitin-mediated protein degradation pathway. During this process, ubiquitin is transferred to Ubc1, thereby forming a transient E2-Ub thiolester complex prior to labeling of the targeted protein. For many E2 proteins this latter step is aided by another enzyme, the E3 ubiquitin ligase. In order to understand the mechanisms underlying the transfer of the ubiquitin molecule to the E2 and then to a targeted protein, it will be necessary to determine the three-dimensional structures of several of the E2-Ub, E3-E2, and E3-E2-Ub complexes. However, the E2-Ub thiolester complex has proven to be elusive due to its transient nature and resistance to complete three-dimensional structure determination by either NMR spectroscopy or X-ray crystallography. In this work, we used NMR spectroscopy to map the interacting surfaces among Ubc1$_{\Delta 450}$, the yeast Ubc1 catalytic domain, and Ub in the transient thiolester complex. The first model of the E2-Ub thiolester complex was then derived from Monte Carlo docking calculations.

In the E2-Ub thiolester, the interface is comprised largely from the "tail" residues L71–G76 from Ub that position themselves in a shallow cleft in the E2 protein formed by residues L89–I91 and N119–P121. Furthermore, these regions in Ub and E2 proteins are highly conserved, indicating that this interaction may be used as a model for other E2-Ub complexes such as that between the human E2 protein, HsUbc2b, and Ub. The E2-Ub complex identified from NMR studies is consistent with recent crystallographic studies of the E2-E3 complexes of UbcH7-c-Cbl and UbcH7-E6AP. Modeling of the Ubc1$_{\Delta 450}$-Ub structure on the UbcH7-c-Cbl indicates that the Ub molecule is adjacent to the E3 protein, thereby providing a rational arrangement of the three proteins for transfer of Ub to a target protein.

Experimental Procedures

Protein Purification

Ub and E2 proteins were expressed in the BL21DE3pLysS *E. coli* strain [7]. His-tagged E1 protein was purified from the *S. cerevisiae* strain JD77.1A (a gift of Dr. Seth Sadis) as previously described. For NMR experiments, ^{15}N-labeling of Ub or E2 was done as described earlier [13].

Thiolester Reactions

All thiolester reactions were performed at 30°C in the NMR tube using 0.8 mM E2 and Ub concentrations with 10 μM E1, 10 mM ATP, 5 mM MgCl in 40 mM HEPES, 450 mM NaCl, and 1 mM EDTA (pH 7.5). Reactions utilized either ^{15}N-Ub and unlabeled E2 or ^{15}N-E2 and unlabeled Ub. Initial ^{1}H-^{15}N HSQC spectra of the ^{15}N-labeled protein were collected. NMR samples were then reduced in volume by Speedvac, and an equimolar amount of unlabeled E2 or Ub was added, thus ensuring that the final volume was identical to that used for the initial spectra (500 μl). ^{1}H-^{15}N HSQC spectra were acquired by using identical parameters to those of the ^{15}N protein alone. The sample volume was then further reduced, and ATP and E1, equilibrated at 30°C, were added to a final volume of 500 μl. The sample was rapidly mixed, transferred to the NMR tube, and an initial spectrum acquired by using the sensitivity-enhanced ^{1}H-^{15}N HSQC method [21]. Spectra of thiolester reactions were acquired every 10 min during the first 60 min of the reaction and were processed with the programs NMRDraw, Pipp, and Stapp [22, 23]. All NMR experiments, and subsequent analyses, were done on a Varian Unity 500 MHz NMR spectrometer at the University of Western Ontario.

X-Ray Crystallography

Initial plate-like crystals of Ubc1$_{\Delta 450}$ were grown at 20°C–22°C by mixing 1 μl of 7 mg/ml Ubc1 in 20 mM HEPES (pH 7.5), 400 mM NaCl, 1 mM EDTA, and 1mM DTT with 1 μl reservoir solution 1 (27% PEG-5000-monomethylether, 9% isopropanol, 100 mM ammonium sulfate, 100 mM MES [pH 6.0], and 5 mM DTT). Improved crystals were obtained by microseeding dilutions of crushed initial crystals into preequilibrated drops containing 5 μl protein solution, and 5 μl reservoir solution 2 (19% PEG-5000-monomethylether, 9% isopropanol, 100 mM ammonium sulfate, 100 mM MES [pH 6.0], and 5 mM DTT). The crystals belong to the space group $P2_1$, with unit cell dimensions a = 42.2 Å, b = 47.5 Å, c = 75.8 Å, $\alpha = 90°$, $\beta = 92.6°$, and $\gamma = 90.0°$. For data collection, crystals were transferred to a cryoprotectant solution containing 19% PEG-5000-monomethylether, 25% glycerol, 100 mM ammonium sulfate, 100 mM MES (pH 6.0), and 5 mM DTT. Diffraction data to 1.9 Å resolution were collected from a single crystal at 105 K with a MacScience DIP2030 image plate detector and rotating anode X-ray generator. Intensity data were processed using DENZO and SCALEPACK [24]. We used molecular replacement, as implemented in the AMORE package [25], to locate the two Ubc1$_{\Delta 450}$ molecules within the crystallographic asymmetric unit. We used a molecular replacement search model based on the yeast Ubc4 structure (Protein Data Bank accession number 2UCE) in which all amino acids in Ubc4 that are not identical to the corresponding residue in Ubc1 were mutated to alanine. Simulated annealing refinement, using torsion angle molecular dynamics, maximum likelihood targets, a bulk solvent correction, and anisotropic B factor correction, as implemented in CNS [26], was used to refine the structure. Manual adjustments to the model were made with the program O [27] with the aid of σ_A-weighted, model-phased, $2|F_o| - |F_c|$ electron density maps and composite simulated annealing omit maps. The model was restrained with 2-fold noncrystallographic symmetry during the early stages of refinement, but these restraints were later removed to accommodate small conformational differences between the two crystallographically independent molecules. The quality of the model was assessed with PROCHECK [28]. The final model contains 2588 atoms, including 300 solvent molecules. Main chain electron density (excluding the cleaved N-terminal methionine) was clearly observed for all residues including loop regions. Side chain electron density was not observed for residues K5, K15, K68, D90, K93, and E135 in molecule A or for residues R3, E57, and K93 in molecule B.

Molecular Modeling

All molecular modeling simulations were performed by using the structure of human Ub (1ubq) [14] and the Ubc1$_{\Delta 450}$ structure reported here. For both molecules, hydrogen atoms were added and default bond orders were fixed. Energy potentials were also calculated, checked, and fixed. Initial side chain minimizations were performed in vacuo (Biopolymer module, Insight II, release 98.0, Biosym Technologies, San Diego, CA), and then both molecules were deposited into a single computational environment.

Ub was then docked to Ubc1$_{\Delta 450}$ in separate Monte Carlo [29] -type energy-comparison experiments, each having 1000 steps containing individual energy minimization calculations (Docking module, Insight II). This analysis resulted in a family of lowest free-energy configurations with approximately common structural features. Within this family, the C terminus of Ub was oriented toward the active site of the E2, and the majority of surface residues on Ub and Ubc1$_{\Delta 450}$ that were affected by thiolester formation (as determined from the HSQC spectra) were brought into proximity. A representative configuration was then manipulated manually to obtain the lowest intermolecular energy without further altering the backbone or side chains of either molecule. Once the initial minimization and dynamics were completed, the thiolester bond was formed between the C88 sulfur on Ubc1$_{\Delta 450}$ and the C-terminal carbon on Ub (Biopolymer module, Insight II). A final round of minimization and dynamics was performed on the entire structure with fixed backbone (Discover 3 module, Insight II) to obtain the final thiolester model shown in Figure 3.

Acknowledgments

We thank Lewis Kay (University of Toronto) for NMR pulse sequences and Frank Delaglio and Dan Garrett (National Institutes of Health) for the programs NMRPipe and Pipp. This research was supported by operating (M.J.E. and G.S.S.) and maintenance (G.S.S.) grants from the Canadian Institutes for Health Research. The NMR spectrometer in the McLaughlin Macromolecular Structure Facility (University of Western Ontario) was purchased through grants from the Medical Research Council of Canada, the Academic Development Fund of the University of Western Ontario, and generous gifts from the R. Samuel McLaughlin Foundation and London Life Insurance Company of Canada.

Received: May 1, 2001
Revised: August 21, 2001
Accepted: August 31, 2001

References

1. Hersko, A., and Ciehanover, A. (1998). The ubiquitin system. Annu. Rev. Biochem. *67*, 425–479.
2. Worthylake, D.K., Prakash, S., Prakash, L., and Hill, C.P. (1998). Crystal structure of the Saccharomyces cerevisiae ubiquitin-conjugating enzyme Rad6 at 2.6 Å resolution. J. Biol. Chem. *273*, 6271–6276.
3. Cook, W.J., Martin, P.D., Edwards, B.F.P., Yamazaki, R.K., and Chau, V. (1997). Crystal structure of a class I ubiquitin conjugating enzyme (Ubc7) from Saccharomyces cerevisiae at 2.9 Å resolution. Biochemistry *36*, 1621–1627.
4. Tong, H., Hateboer, G., Perrakis, A., Bernards, R., and Sixma, T.K. (1997). Crystal structure of murine/human Ubc9 provides insight into the variability of the ubiquitin-conjugating system. J. Biol. Chem. *272*, 21381–21387.
5. Huang, L., et al., and Pavletich, N.P. (1999). Structure of an E6AP-UbcH7 complex: insights into ubiquitination by the E2-E3 enzyme cascade. Science *286*, 1321–1326.
6. Zheng, N., Wang, P., Jeffrey, P.D., and Pavletich, N.P. (2000). Structure of a c-Cbl-UbcH7 complex: RING domain function in ubiquitin-protein ligases. Cell *102*, 533–539.
7. Hodgins, R., Gwozd, C., Arnason, R., Cummings, M., and Ellison, M.J. (1996). The tail of a ubiquitin-conjugating enzyme redirects multi-ubiquitin chain synthesis from the lysine 48-linked configuration to a novel nonlysine-linked form. J. Biol. Chem. *271*, 28766–28771.
8. Wilkinson, K.D., et al., and Wand, A.J. (1999). The binding site for UCH-L3 on ubiquitin: mutagenesis and NMR studies on the complex between ubiquitin and UCH-L3. J. Mol. Biol. *291*, 1067–1077.
9. Rajesh, S., Sakamoto, T., Iwamoto-Sugai, M., Shibata, T., Kohno, T., and Ito, Y. (1999). Ubiquitin binding interface mapping

on yeast ubiquitin hydrolase by NMR chemical shift perturbation. Biochemistry *38*, 9242–9253.
10. Liu, Q., Jin, C., Liao, X., Shen, Z., Chen, D.J., and Chen, Y. (1999). The binding interface between an E2 (UBC9) and a ubiquitin homologue (UBL1). J. Biol. Chem. *274*, 16979–16987.
11. Miura, T., Klaus, W., Gsell, B., Miyamoto, C., and Senn, H. (1999). Characterization of the binding interface between ubiquitin and class I human ubiquitin-conjugating enzyme 2b by multidimensional heteronuclear NMR spectroscopy in solution. J. Mol. Biol. *290*, 213–228.
12. Hamilton, K.S., Ellison, M.J., and Shaw, G.S. (2000). Identification of the ubiquitin interfacial residues in a ubiquitin-E2 covalent complex. J. Biomol. NMR *18*, 319–327.
13. Hamilton, K.S., Ellison, M.J., and Shaw, G.S. (2000). 1H, 15N and 13C resonance assignments for the catalytic domain of the yeast E2, UBC1. J. Biomol. NMR *16*, 351–352.
14. Vijay-Kumar, S., Bugg, C.E., and Cook, W.J. (1987). Structure of ubiquitin refined at 1.8 A resolution. J. Mol. Biol. *194*, 531–544.
15. Wand, A.J., Urbauer, J.L., McEvoy, R.P., and Bieber, R.J. (1996). Internal dynamics of human ubiquitin revealed by 13C-relaxation studies of randomly fractionally labeled protein. Biochemistry *35*, 6116–6125.
16. Schneider, D.M., Dellwo, M.J., and Wand, A.J. (1992). Fast internal main-chain dynamics of human ubiquitin. Biochemistry *31*, 3645–3652.
17. Ecker, D.J., et al., and Crooke, S.T. (1987). Gene synthesis, expression, structures, and functional activities of site-specific mutants of ubiquitin. J. Biol. Chem. *262*, 14213–14221.
18. Burch, T.J., and Haas, A.L. (1994). Site-directed mutagenesis of ubiquitin. Differential roles for arginine in the interaction with ubiquitin-activating enzyme. Biochemistry *33*, 7300–7308.
19. Beal, R., Deveraux, Q., Xia, G., Rechsteiner, M., and Pickart, C. (1996). Surface hydrophobic residues of multiubiquitin chains essential for proteolytic targeting. Proc. Natl. Acad. Sci. USA *93*, 861–866.
20. Nuber, U., and Scheffner, M. (1999). Identification of determinants in E2 ubiquitin-conjugating enzymes required for hect E3 ubiquitin-protein ligase interaction. J. Biol. Chem. *274*, 7576–7582.
21. Kay, L.E., Keifer, P., and Saarinen, T. (1992). Pure absorption gradient enhanced heteronuclear single quantum correlation spectroscopy with improved sensitivity. J. Am. Chem. Soc. *114*, 10663–10665.
22. Delaglio, F., Grzesiek, S., Vuister, G.W., Zhu, G., Pfeifer, J., and Bax, A. (1995). NMRPipe: a multidimensional spectral processing system based on UNIX pipes. J. Biomol. NMR *6*, 277–293.
23. Garrett, D.S., Powers, R., Gronenborn, A.M., and Clore, G.M. (1991). A common sense approach to peak picking in two-, three-, and four-dimensional spectra using automatic computer analysis of contour diagrams. J. Magn. Reson. *95*, 214–220.
24. Otwinowski, Z., and Minor, W. (1997). Processing of x-ray diffraction data collected in oscillation mode. In Methods in Enzymology, Volume 276, C.W. Carter, Jr. and R.M. Sweet, eds. (New York: Academic Press), pp. 307–326.
25. Navaza, J. (1994). AMORE—an automated package for molecular replacement. Acta Crystallogr. A *50*, 157–163.
26. Brünger, A.T., et al., and Warren, G.L. (1998). Crystallography and NMR System—a new software suite for macromolecular structure determination. Acta Crystallogr. D *54*, 905–921.
27. Jones, T.A., Zhou, J.-Y., Cowan, S.W., and Kjeldgaard, M. (1991). Improved methods for building protein models in electron density maps and the location of errors in these models. Acta Crystallogr. A *A47*, 110–119.
28. Laskowski, R.A., MacArthur, M.W., Moss, D.S., and Thornton, J.M. (1993). PROCHECK: a program to check the stereochemical quality of protein structures. J. Appl. Crystallogr. *26*, 283–291.
29. Hart, T.N., and Reid, R.J. (1992). A multiple-start Monte Carlo docking method. Proteins *13*, 206–222.

Accession Numbers

Coordinates for the crystallographic structure of $Ubc1_{\Delta 450}$ and the model for the E2-Ub thiolester have been deposited in the Protein Data Bank (1FXT and RCSB011993, respectively).